Poincare Journal of Analysis & Applications
Vol. 11, No. 1 (2024), 67-84
©*Poincare Publishers*
DOI: 10.46753/pjaa.2024.v011i01.005
Online Published on 22. 06. 2024

ON S-ELEMENTARY WAVELETS IN $\mathbb{R}$ AND THEIR APPLICATIONS IN SOLVING INTEGRAL EQUATIONS

M. J. KHEIRDEH, A. ASKARI HEMMAT, AND H. SAEEDI†

Date of Receiving : 26. 12. 2023
Date of Acceptance : 18. 03. 2024

Abstract. In this paper, we introduce a class of s-elementary wavelets as the basis functions and use them to present an operational computational method for solving nonlinear Fredholm and Volterra integral equations. For presenting the methods, first, operational matrices for the s-elementary wavelets are derived. Then, the s-elementary wavelets bases along with these operational matrices are applied for solving integral equations. Convergence analysis of the s- elementary wavelets basis are investigated. To reveal the accuracy and efficiency of the proposed method some numerical examples are included and the obtained results are compared with some references.

1. Introduction

The word wavelet was first introduced by Haar in 1909 and it was developed by Chui [5], Daubechies [9], Dai and Lu [8], Meyer[22], Fang and Wang [10] and Hernandez and Weiss [14]. A special type of wavelet that is called s-elementary wavelet, first introduced by Dai and Larson [6] also, Gabardo and Yu [11] and Benedetto and Sumetkijakan [2], have come up with new and different ways to build these wavelet sets.
In recent years, integral theory has attracted much more attention from physicists and mathematicians. In fact there are many problems in physics, mechanics, chemistry and biology that are in the form of partial differential equations, linear and nonlinear integral equations. There are several methods for solving these types of equations as the polynomial approximation [28], linear multistep methods [3], modified homotopy perturbation [12, 29], wavelets [31], triangular functions [27], Newton–Kantorovich method [24] and the Haar wavelet method and the higher order Haar wavelet method

---

2010 *Mathematics Subject Classification.* 42C15.
Key words and phrases. Wavelet sets; s-elementary wavelets; Integral equations; Operational matrix.
The second author would like to thank Concordia University for hosting and providing facilities during the sabbatical period from September 2023 to June 2024.
Communicated by: Neyaz Ahmad Sheikh
† *Corresponding author*

[4, 15, 17, 18, 19, 20, 21, 23, 30].
In section 2, we will recall wavelets and introduce s-elementary wavelets and using them to create a suitable wavelet basis for solution of integral equations.
Section 3 is devoted to introduce s-elementary wavelets operational matrices and how to find its entries.
In section 4, we will analyze the convergence of s-elementary wavelets approximation series.
In the last section, we use of s-elementary wavelets for numerical solution of Fredholm and Volterra integral equations and compare the results with the previous methods. Furthermore, for a better understanding of the concept of wavelet sets, we have provided two examples, in case n=2, in the appendix.

2. Wavelet sets and bases

Assuming that the reader is familiar with the content of wavelet analysis. We have provided the definitions and main content of this section from references [6, 7, 14].

Definition 2.1. The function $\psi \in L^2(\mathbb{R})$ is called a 2-dilation wavelet, if the set $\{\psi_{jm}\}_{j,m\in\mathbb{Z}}$ is an orthonormal basis for $L^2(\mathbb{R})$, here ψ_{jm} is defined by $\psi_{jm}(x) := 2^{\frac{j}{2}}\psi(2^j x - m)$.

Definition 2.2. Let $\{V_j\}_{j\in\mathbb{Z}}$ be a sequence of closed subspaces of functions in $L^2(\mathbb{R})$. The collection of spaces $\{V_j\}_{j\in\mathbb{Z}}$ is called a Multiresolution Analysis (MRA) $L^2(\mathbb{R})$ if the following conditions hold,
1. $V_j \subset V_{j+1}$ for all $j \in \mathbb{Z}$,
2. $f(.) \in V_j$ iff $f(2.) \in V_{j+1}$ for all $j \in \mathbb{Z}$,
3. $\bigcap_{j\in\mathbb{Z}} V_j = \{0\}$ and $\bigcup_{j\in\mathbb{Z}} V_j$ is dense in $L^2(\mathbb{R})$,
4. $f(.) \in V_0$ iff $f(. - n) \in V_0$ for all $n \in \mathbb{Z}$,
5. There exists a function $\varphi \in V_0$, called the **scaling function**, such that the family $\{\varphi(. - m);\ m \in \mathbb{Z}\}$ is an orthonormal basis for V_0.

Definition 2.3. If $f, g \in L^1(\mathbb{R}) \cap L^2(\mathbb{R})$ then the Fourier transform of f is defined by $\hat{f}(\xi) = \int_{-\infty}^{\infty} f(x)\, e^{-i\xi x} dx$ and the inverse Fourier transform of g by $\check{g}(x) = \frac{1}{2\pi}\int_{-\infty}^{\infty} g(\xi)\, e^{i\xi x} d\xi$.

Lemma 2.4. [14] *Let φ be the scaling function of an MRA and let ψ be the corresponding wavelet function. Then $|\hat{\varphi}(\xi)|^2 = \sum_{j=0}^{+\infty} |\hat{\psi}(2^j\xi)|^2$, a.e $\xi \in \mathbb{R}$.*

Definition 2.5. [7] The measurable subset $W \subset \mathbb{R}$, with finite measure, is a **wavelet set** for $L^2(\mathbb{R})$ if the inverse Fourier transform of $\hat{\psi} = \chi_W$ be an orthonormal wavelet for $L^2(\mathbb{R})$.

Note. We are following Dai and Larson [6, 7] and call this type of wavelets, **s-elementary wavelets**. (The prefix "s" is for "set".)

Corollary 2.6. [10] Let $W \subset \mathbb{R}$ be a measurable set and $\hat{\psi} = \chi_W$ then ψ is an orthonormal wavelet if and only if $\{2^j W;\ j \in \mathbb{Z}\}$ and $\{W + 2\pi m;\ m \in \mathbb{Z}\}$ are both partitions of $\mathbb{R}$.

Example 2.7. In [13], it is proved that $W_c = [4\pi(c-1),\ 2\pi(c-1)) \cup (2\pi c,\ 4\pi c]$, where $c \in (0,\ 1)$, is a 2−dilation wavelet set. For $c = 0.5$, $W_{0.5} = [-2\pi,\ -\pi) \cup (\pi,\ 2\pi]$ is the **Shannon** wavelet set (see Figure 1).

By Lemma 2.4, the scaling function for χ_{W_c} is of the form χ_{Q_c}, with $Q_c = [2\pi(c-1),\ 2\pi c]$. Now, we put:

$$ {}_c\,\hat{\varphi}\,(x) = \begin{cases} \frac{1}{\sqrt{2\pi}}, & x \in [2\pi(c-1),\ 2\pi c]\,, \\ 0, & other\ wise. \end{cases} \tag{2.1} $$

Corollary 2.8. [16] If we define ${}_c\,\hat{\varphi}_{mk}\,(x) := \frac{2^{\frac{k}{2}}}{\sqrt{2\pi}}\ {}_c\,\hat{\varphi}\left(2^k x - 2m\pi\right)$ for $k, m \in \mathbb{Z}$ and $c \in (0,\ 1)$ where ${}_c\,\hat{\varphi}$ is defined as in (2.1), then for fix k, the system $\{{}_c\,\hat{\varphi}_{mk}\ ;\ m \in \mathbb{Z}\}$ is an orthonormal basis for $L^2(\mathbb{R})$.

By Definition 2.5 the inverse Fourier transform of χ_{W_c} is an orthonormal s-elementary wavelet. Now, we put:

$$ {}_c\,\hat{\psi}\,(x) = \begin{cases} \frac{1}{\sqrt{2\pi}}, & x \in [4\pi(c-1),\ 2\pi(c-1)) \cup (2\pi c,\ 4\pi c]\,, \\ 0, & other\ wise. \end{cases} $$

If we define ${}_c\,\hat{\psi}_{mk}\,(x) := \frac{2^{\frac{k}{2}}}{\sqrt{2\pi}}\ {}_c\,\hat{\psi}\left(2^k x - 2m\pi\right)$ for $k, m \in \mathbb{Z}$ and $c \in (0,\ 1)$.

In [16], the authors showed for fix k, the system $\left\{{}_c\,\hat{\psi}_{mk}\ ;\ m \in \mathbb{Z}\right\}$ is an orthonormal basis for $L^2(\mathbb{R})$.
In [13] , a generalization of the beautiful concept of wavelet sets has been provided in a more general form in $L^2(\mathbb{R}^n)$.

Theorem 2.9. *(Hernandez and Weiss) Let A be an expansive matrix and let $E \subset \mathbb{R}^n$ be a measurable set. Then E is a wavelet set if and only if E is both an A-dilation generator of a partition (modulo null sets) of $\mathbb{R}^n$ and a 2π-translation ($\mathbb{Z}^n$-translation) generator of a partition (modulo null sets) of $\mathbb{R}^n$.* ■

In Figure 1, for the case of n=1, the wavelet set (a), scaling function (b) and the corresponding wavelet (c) have been plotted.

In the Appendix, two examples have been presented for the case of n=2.

3. S-elementary wavelets operational matrices

From now on, consider k as a fixed number unless it is mentioned as something else.

Let ${}_{(c)}\hat{\Psi}_{mk}$ be the vector of s-elementary wavelets, so we put:

$$ {}_{(c)}\hat{\Psi}_{mk} := \left[{}_c\,\hat{\psi}_{0k},\ {}_c\,\hat{\psi}_{1k},\ {}_c\,\hat{\psi}_{2k}, ...,\ {}_c\,\hat{\psi}_{mk}\right]^T. \tag{3.1} $$

As a consequence of definition (3.1), we can obtain appropriate approximation of functions in $L^2[0,1]$, if we choose k large enough. Also using large k's one can cover the

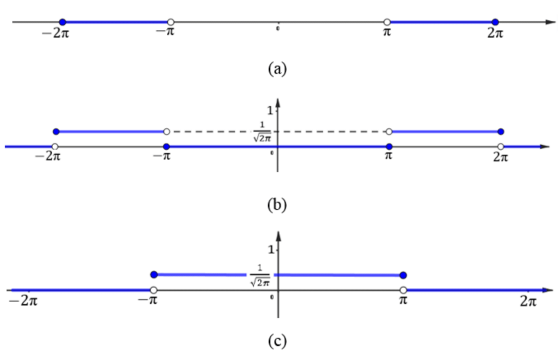

FIGURE 1. Shannon wavele, (a) wavelet set, (b) scaling function, (c) wavelet associated to n=1 in Theorem 2.9.

interval $[0,1]$ with the union of supports of ${}_c\hat{\psi}_{mk}$'s i. e. $V = \cup_{i=0}^{m}\ supp\left({}_c\hat{\psi}_{ik}\right)$ so that the measure of $V\backslash[0,1]$ be smaller than every $\epsilon > 0$. Then for $f \in L^2[0,1]$, we have:

$$f \simeq \sum_{i=0}^{m} d_{ik}\ {}_c\ \hat{\psi}_{ik} = D^T\, {}_{(c)}\hat{\Psi}_{mk}, \tag{3.2}$$

where $d_{ik} = \left\langle f,\ {}_c\ \hat{\psi}_{ik}\right\rangle$, $D^T = [d_{0k}, d_{1k}, ..., d_{mk}]$ and $\langle .,\ .\rangle$ is an inner product on $L^2[0,1]$.

Lemma 3.1. [16] *Let* ${}_{(c)}\hat{\Psi}_{mk}$ *is the vector of s-elementary wavelets in* (3.1). *The integration of its entries can be expanded as follows,*

$$\int_0^x {}_{(c)}\hat{\Psi}_{mk}(t)\, dt = {}_{(c)}\hat{P}\ {}_{(c)}\hat{\Psi}_{mk}(x), \tag{3.3}$$

where the $(m+1)\times(m+1)$ *matrix* ${}_{(c)}\hat{P} = [{}_{(c)}\hat{p}_{ij}]$ *is called the operational matrix of s-elementary wavelets and its entries are:*

$$ {}_{(c)}\hat{p}_{ij} = \left\langle \int_0^{(.)} {}_c\hat{\psi}_{i-1,k}(t)dt,\ {}_c\hat{\psi}_{j-1,k} \right\rangle.$$

For $a = \frac{\pi}{2^k}$, *the* $(m+1)\times(m+1)$ *operational matrix of s-elementary wavelets is as the following,*

$${}_{(c)}\hat{P}^{k}_{(m+1)} = \begin{bmatrix} a & a(2c^2-2c+2) & 2a & \dots & 2a & 2a \\ 2a(c-c^2) & a & a(2c^2-2c+2) & 2a & \dots & 2a \\ 0 & 2a(c-c^2) & a & a(2c^2-2c+2) & \dots & 2a \\ \vdots & \ddots & \ddots & \ddots & \ddots & \vdots \\ 0 & \dots & 2a(c-c^2) & a & a(2c^2-2c+2) & 2a \\ 0 & 0 & \dots & 0 & 2a(c-c^2) & a \end{bmatrix}.$$

As an example, for $c = 0.5$ and $m = 4$, the above matrix takes the following form,

$$
{}_{(0.5)}\hat{P}^{k}_{(5)} = \begin{bmatrix} a & \frac{3a}{2} & 2a & 2a & 2a \\ \frac{a}{2} & a & \frac{3a}{2} & 2a & 2a \\ 0 & \frac{a}{2} & a & \frac{3a}{2} & 2a \\ 0 & 0 & \frac{a}{2} & a & \frac{3a}{2} \\ 0 & 0 & 0 & \frac{a}{2} & a \end{bmatrix}_{(5\times 5)}.
$$

We put:

$$
{}_{(c)}\hat{\Phi}_{mk} = [{}_c\,\hat{\varphi}_{0k},\ {}_c\,\hat{\varphi}_{1k},\ {}_c\,\hat{\varphi}_{2k}, ...,\ {}_c\,\hat{\varphi}_{mk}]^T, \tag{3.4}
$$

similar to the description in the second paragraph at the beginning of this section, for $f \in L^2[0,1]$, we have:

$$
f \simeq \sum_{i=0}^{m} h_{ik}\ {}_c\,\hat{\varphi}_{ik} = H^T\,{}_{(c)}\hat{\Phi}_{mk}, \tag{3.5}
$$

where $h_{ik} = \langle f,\ {}_c\,\hat{\varphi}_{ik}\rangle$, $H^T = [h_{0k}, h_{1k}, ..., h_{mk}]$.

Lemma 3.2. [16] *Let ${}_{(c)}\hat{\Phi}_{mk}$ be the vector of s-elementary wavelets in (3.4). The integration of its entries can be expanded as follows,*

$$
\int_0^x {}_{(c)}\hat{\Phi}_{mk}(t)\,dt = {}_{(c)}\hat{Q}\ {}_c\hat{\Phi}_{mk}(x), \tag{3.6}
$$

where the $(m+1)\times(m+1)$ matrix ${}_{(c)}\hat{Q} = [{}_{(c)}\hat{q}_{ij}]$ is called the operational matrix of s-elementary wavelets and its entries are:

$$
{}_{(c)}\hat{q}_{ij} = \left\langle \int_0^{(.)} {}_c\,\hat{\varphi}_{i-1,k}(t)dt,\ {}_c\,\hat{\varphi}_{j-1,k} \right\rangle.
$$

We put $a = \frac{\pi}{2^k}$, the $(m+1)\times(m+1)$ operational matrix of s-elementary wavelets is as the following:

$$
{}_{(c)}\hat{Q}^{k}_{(m+1)} = \begin{bmatrix} a & 2a & \cdots & 2a & 2a \\ 0 & a & 2a & \cdots & 2a \\ \vdots & \ddots & \ddots & \ddots & \vdots \\ 0 & \cdots & \ddots & a & 2a \\ 0 & 0 & \cdots & 0 & a \end{bmatrix}_{(m+1)\times(m+1)}.
$$

Lemma 3.3. *Let $E = [e_0, e_1, ..., e_m]^T$ be a vector and $\omega = \frac{2^{\frac{k}{2}}}{\sqrt{2\pi}}$. Then we have the following relationships:*

$$
E^T\ {}_{(c)}\hat{\Psi}_{mk}\ {}_{(c)}\hat{\Psi}^T_{mk} = {}_{(c)}\hat{\Psi}^T_{mk} diag(\omega E), \tag{3.7}
$$

$$
\int_0^1 {}_{(c)}\hat{\Psi}_{mk}(x)dx = \frac{1}{\omega}[1, 1, \cdots, 1]^T_{(m+1)\times 1}, \tag{3.8}
$$

$$
E^T\ {}_{(c)}\hat{\Phi}_{mk}\ {}_{(c)}\hat{\Phi}^T_{mk} = {}_{(c)}\hat{\Phi}^T_{mk} diag(\omega E), \tag{3.9}
$$

$$\int_0^1 {}_{(c)}\hat{\Phi}_{mk}(x)dx = \frac{1}{\omega}[1, 1, \cdots, 1]^T{}_{(m+1)\times 1}. \tag{3.10}$$

Proof. It is easy to prove it. □

4. Convergence analysis

Theorem 4.1. *Let $\sum_{i=0}^{\infty} d_{ik}\ {}_c\,\hat{\psi}_{ik}$ be the s-elementary wavelets series of $f \in L^2[0,1]$, then $f_m = \sum_{i=0}^{m} d_{ik}\ {}_c\,\hat{\psi}_{ik}$ convergences to f as $m \to +\infty$.*

Proof. By using relation (3.2), we have:

$$d_{ik} = \left\langle f,\ {}_c\,\hat{\psi}_{ik} \right\rangle. \tag{4.1}$$

First we will show that the sequence of partial sums $\sum_{i=0}^{\infty} d_{ik}\ {}_c\,\hat{\psi}_{ik}$, f_m, is a Cauchy sequence in the Hilbert space of $L^2[0,1]$. Let f_m be an arbitrary partial sums of $\sum_{i=0}^{\infty} d_{ik}\ {}_c\,\hat{\psi}_{ik}$, i.e., $f_m = \sum_{i=0}^{m} d_{ik}\ {}_c\,\hat{\psi}_{ik}$, also $p > m$, then we get:

$$\begin{aligned}
||f_m - f_p||^2 &= \left|\left| \sum_{i=m+1}^{p} d_{ik}\ {}_c\,\hat{\psi}_{ik} \right|\right|^2 \\
&= \left\langle \sum_{i=m+1}^{p} d_{ik}\ {}_c\,\hat{\psi}_{ik},\ \sum_{j=m+1}^{p} d_{jk}\ {}_c\,\hat{\psi}_{jk} \right\rangle \\
&= \sum_{i=m+1}^{p} \sum_{j=m+1}^{p} d_{ik} d_{jk} \left\langle {}_c\,\hat{\psi}_{ik},\ {}_c\,\hat{\psi}_{jk} \right\rangle \\
&= \sum_{i=m+1}^{p} |d_{ik}|^2 .
\end{aligned}$$

By Bessel inequality, we have:

$$\sum_{i=m+1}^{p} |d_{ik}|^2 \leq \sum_{i=0}^{\infty} |d_{ik}|^2 \leq ||f||^2 < \infty.$$

Thus, $||f_m - f_p||^2 \to 0$ as m,p $\to +\infty$, that is, f_m is a Cauchy sequence, hence f_m converges to some $g \in L^2[0,1]$. Finally we show that $g = f$. For k large enough and by using relation (4.1) and property of continuity of inner product, we get:

$$\begin{aligned}
\left\langle g - f,\ {}_c\,\hat{\psi}_{ik} \right\rangle &= \left\langle g,\ {}_c\,\hat{\psi}_{ik} \right\rangle - \left\langle f,\ {}_c\,\hat{\psi}_{ik} \right\rangle \\
&= \lim_{m\to+\infty} \left\langle f_m,\ {}_c\,\hat{\psi}_{ik} \right\rangle - d_{ik} \\
&= d_{ik} - d_{ik} \\
&= 0,
\end{aligned}$$

hence $g = f$ and the proof is completed. □

Note that, the above theorem is correct for $\sum_{i=0}^{\infty} h_{ik}\ {}_c\,\hat{\varphi}_{ik}$.

5. Main Results

In this section, we present an operational method for solving a class of nonlinear Fredholm and Volterra integral equations by using the s-elementary wavelets as an application of them.
If u is the exact solution of an integral equation, fix k and consider $u_k = \sum_{i=0}^{m} d_{ik\ c}\ \hat{\psi}_{ik}$ as the approximate solution. Then the experimental rate of convergence, $R_k(x)$, can be estimated as follows:

$$R_k(x) = \log \left| \frac{u_{k+1}(x) - u(x)}{u_k(x) - u(x)} \right|, \text{ for } k = 1,\ 2,\ 3, \dots .$$

Remark. For different values of c, the error rate is not so significant. Table 2 shows changing c will give better accuracy for some x values and less accuracy for some other values. But in general, increasing the value of k, for a fixed c, increases the accurate.

5.1. Numerical solution of Fredholm integral equations. Consider the following nonlinear Fredholm integral equation of the second kind,

$$u(t) = f(t) + \int_0^1 K(t,s) \sum_{l=0}^{N} f_l(s) u^l(s) ds, \ N > 1, \tag{5.1}$$

where the functions $f, f_l \in L^2[0,1]$ and $K(t,s) \in L^2([0,1] \times [0,1])$ are given functions, $u(t)$ is unknown function and N is a positive integer. Note that in Eq. (5.1), for $N = 1$ the equation is linear and otherwise nonlinear, which are given in examples (5.1) and (5.2). Here, we suppose that $K(t,s) = k_1(t) k_2(s)$. By Eq. (3.2) we get:

$$f \simeq F^T{}_{(c)}\hat{\Psi}_{mk},\ f_l \simeq F_l^T{}_{(c)}\hat{\Psi}_{mk},\ k_1 \simeq K_1^T{}_{(c)}\hat{\Psi}_{mk}, k_2 \simeq K_2^T{}_{(c)}\hat{\Psi}_{mk},\ u \simeq U^T{}_{(c)}\hat{\Psi}_{mk}. \tag{5.2}$$

By substitute Eqs. (5.2) into (5.1) and by Eq. (3.7) we have:

$$\begin{aligned}
&U^T{}_{(c)}\hat{\Psi}_{mk}(t) = F^T{}_{(c)}\hat{\Psi}_{mk}(t) + \\
&\int_0^1 K_1^T{}_{(c)}\hat{\Psi}_{mk}(t) K_2^T{}_{(c)}\hat{\Psi}_{mk}(s) \sum_{l=0}^{N} F_l^T{}_{(c)}\hat{\Psi}_{mk}(s) \left(U^T{}_{(c)}\hat{\Psi}_{mk}(s)\right)^l (s) ds \\
&= F^T{}_{(c)}\hat{\Psi}_{mk}(t) + \\
&\int_0^1 K_1^T{}_{(c)}\hat{\Psi}_{mk}(t) K_2^T{}_{(c)}\hat{\Psi}_{mk}(s) \sum_{l=0}^{N} F_l^T{}_{(c)}\hat{\Psi}_{mk}(s) {}_{(c)}\hat{\Psi}^T_{mk}(s)\ diag\left(\omega^{l-1}\ U^{l-1}\right) U ds \\
&= F^T{}_{(c)}\hat{\Psi}_{mk}(t) + \\
&\int_0^1 K_1^T{}_{(c)}\hat{\Psi}_{mk}(t) K_2^T{}_{(c)}\hat{\Psi}_{mk}(s) \sum_{l=0}^{N} {}_{(c)}\hat{\Psi}^T_{mk}(s)\ diag\left(\omega F_l\right)\ diag\left(\omega^{l-1}\ U^{l-1}\right) U ds \\
&= F^T{}_{(c)}\hat{\Psi}_{mk}(t) + \\
&\int_0^1 K_1^T{}_{(c)}\hat{\Psi}_{mk}(t) \sum_{l=0}^{N} {}_{(c)}\hat{\Psi}^T_{mk}(s)\ diag\left(\omega K_2\right)\ diag\left(\omega F_l\right)\ diag\left(\omega^{l-1}\ U^{l-1}\right) U ds \\
&= F^T{}_{(c)}\hat{\Psi}_{mk}(t) + {}_{(c)}\hat{\Psi}_{mk}(t) K_1^T \times \\
&\int_0^1 \left(\sum_{l=0}^{N} {}_{(c)}\hat{\Psi}^T_{mk}(s)\ diag\left(\omega K_2\right)\ diag\left(\omega F_l\right)\ diag\left(\omega^{l-1}\ U^{l-1}\right) U\right) ds.
\end{aligned}$$

Now, by taking transpose on both sides of above equation, we get:

$$
{}_{(c)}\hat{\Psi}^{T}_{mk}(t)U = {}_{(c)}\hat{\Psi}^{T}_{mk}(t)F + {}_{(c)}\hat{\Psi}^{T}_{mk}(t)K_1 \times
$$
$$
\left(\sum_{l=0}^{N} U^T \ diag\left(\omega K_2\right) \ diag\left(\omega F_l\right) \ diag\left(\omega^{l-1} \ U^{l-1}\right) U\right) \int_0^1 {}_{(c)}\hat{\Psi}_{mk}(s)ds
$$

$$
U = F + K_1 \times
$$
$$
\left(\sum_{l=0}^{N} U^T \ diag\left(\omega K_2\right) \ diag\left(\omega F_l\right) \ diag\left(\omega^{l-1} \ U^{l-1}\right) U\right) \int_0^1 {}_{(c)}\hat{\Psi}_{mk}(s)ds
$$

$$
U = F + K_1 \times
$$
$$
\left(\sum_{l=0}^{N} U^T \ diag\left(\omega K_2\right) \ diag\left(\omega F_l\right) \ diag\left(\omega^{l-1} \ U^{l-1}\right) U\right) \ \frac{1}{\omega} \ [1, 1, \cdots, 1]^T. \tag{5.3}
$$

Eq. (5.3) is a system of nonlinear algebraic equations, with unknown vector U. We solve this nonlinear system by the Newton method and obtain u as $u \simeq U^T {}_{(c)}\hat{\Psi}_{mk}$. Note that the above method can be stated by basis vector (3.4).

Example 5.1. Consider the following nonlinear Fredholm equation [24, 25],

$$
u(t) = sin(\pi t) + \frac{1}{5} \int_0^1 cos(\pi t) sin(\pi s) u^3(s)ds, \tag{5.4}
$$

the exact solution of this equation is $u(t) = sin(\pi t) + \frac{1}{3}(20 - \sqrt{391})cos(\pi t)$. In Table 1, we compare our error approximations with the methods in [24, 25] and in Table 2, we did it for different values of c. Fig. 2, (a) and (b) show the comparisons between the approximate solutions and exact solutions, when we used ${}_{(c)}\hat{\Phi}_{mk}$ and ${}_{(c)}\hat{\Psi}_{mk}$ in our method, respectively.

Table 1: Absolute error comparison of the present method with the methods in [24, 25] (Example: 5.1).

x	[24]	[25] $N = 16$	New method by ${}_{(0.5)}\hat{\Psi}_{m,16}(x)$	New method by ${}_{(0.5)}\hat{\Phi}_{m,16}(x)$
0.1	4.74×10^{-2}	1.94×10^{-4}	2.68×10^{-4}	1.07×10^{-5}
0.2	4.03×10^{-2}	2.15×10^{-2}	2.12×10^{-4}	1.79×10^{-5}
0.3	2.93×10^{-2}	5.63×10^{-4}	1.41×10^{-4}	1.81×10^{-5}
0.4	1.54×10^{-2}	1.26×10^{-3}	6.05×10^{-5}	1.09×10^{-5}
0.5	0	1.32×10^{-3}	1.85×10^{-5}	4.30×10^{-6}
0.6	1.54×10^{-2}	1.23×10^{-3}	8.86×10^{-5}	2.61×10^{-5}
0.7	2.93×10^{-2}	3.08×10^{-4}	1.43×10^{-4}	5.18×10^{-5}
0.8	4.03×10^{-2}	1.39×10^{-3}	1.79×10^{-4}	7.79×10^{-5}
0.9	4.74×10^{-2}	4.96×10^{-5}	1.93×10^{-4}	1.001×10^{-4}

Example 5.2. Consider the following nonlinear Fredholm equation [1, 24],

$$
u(t) + \int_0^1 e^{t-2s} u^3(s)ds = e^{t+1}, \tag{5.5}
$$

Table 2: Absolute error comparison of the present method for different values of c (Example: 5.1).

x	${}_c\hat{\Psi}_{m,10}(x)$ $c=0.11$	${}_c\hat{\Psi}_{m,10}(x)$ $c=0.99$	${}_c\hat{\Phi}_{m,10}(x)$ $c=0.3$	${}_c\hat{\Phi}_{m,10}(x)$ $c=0.8$
0.1	9.52×10^{-3}	3.54×10^{-3}	8.93×10^{-3}	2.62×10^{-5}
0.2	3.45×10^{-3}	1.46×10^{-3}	2.99×10^{-3}	1.03×10^{-2}
0.3	6.58×10^{-4}	4.06×10^{-3}	9.61×10^{-4}	4.09×10^{-3}
0.4	6.59×10^{-3}	1.36×10^{-3}	1.83×10^{-3}	4.82×10^{-4}
0.5	5.75×10^{-4}	2.99×10^{-5}	8.95×10^{-4}	2.50×10^{-4}
0.6	3.97×10^{-4}	2.08×10^{-3}	1.21×10^{-4}	3.83×10^{-3}
0.7	3.07×10^{-3}	5.21×10^{-3}	3.51×10^{-3}	2.72×10^{-3}
0.8	3.48×10^{-3}	1.92×10^{-3}	9.51×10^{-3}	1.31×10^{-3}
0.9	2.92×10^{-3}	3.39×10^{-3}	2.29×10^{-3}	1.17×10^{-2}

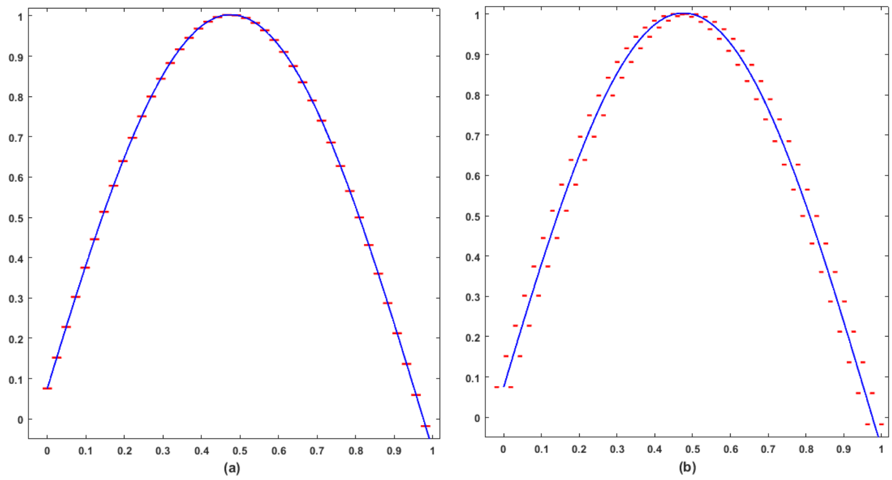

FIGURE 2. Comparison of the approximated solution (dashed red line) using ${}_{(0.5)}\hat{\Phi}_{m,8}$ (a) and ${}_{(0.5)}\hat{\Psi}_{m,8}$ (b) with the exact solution (blue line) (Example: 5.1).

the exact solution of this equation is $u(t) = e^t$. In Table 3, we compare our error approximations with the methods in [1, 24] and in Table 4, we compute the rate of convergence for some k. Fig. 3, (a) and (b) show the comparisons between the approximate solutions and exact solutions, when we used ${}_{(c)}\hat{\Phi}_{mk}$ and ${}_{(c)}\hat{\Psi}_{mk}$ in our method, respectively.

Table 3: Absolute error comparison of the present method with the methods in [1, 24] (Example: 5.2).

x	[1]	[24] $N=16$	New method by ${}_{(0.3)}\hat{\Psi}_{i,16}(x)$	New method by ${}_{(0.3)}\hat{\Phi}_{i,16}(x)$
0.1	2.05×10^{-3}	4.31×10^{-4}	8.77×10^{-5}	1.81×10^{-5}
0.2	3.30×10^{-3}	3.32×10^{-7}	9.25×10^{-5}	2.42×10^{-5}
0.3	8.69×10^{-3}	7.91×10^{-4}	9.73×10^{-5}	3.21×10^{-5}
0.4	1.69×10^{-2}	2.92×10^{-4}	1.02×10^{-4}	4.09×10^{-5}
0.5	1.87×10^{-2}	1.29×10^{-3}	1.06×10^{-4}	5.12×10^{-5}
0.6	1.17×10^{-2}	7.11×10^{-4}	1.11×10^{-4}	6.32×10^{-5}
0.7	2.93×10^{-3}	5.49×10^{-7}	1.15×10^{-4}	7.71×10^{-5}
0.8	8.08×10^{-3}	1.30×10^{-3}	1.02×10^{-4}	9.33×10^{-5}
0.9	2.16×10^{-2}	4.81×10^{-4}	1.23×10^{-4}	1.12×10^{-4}

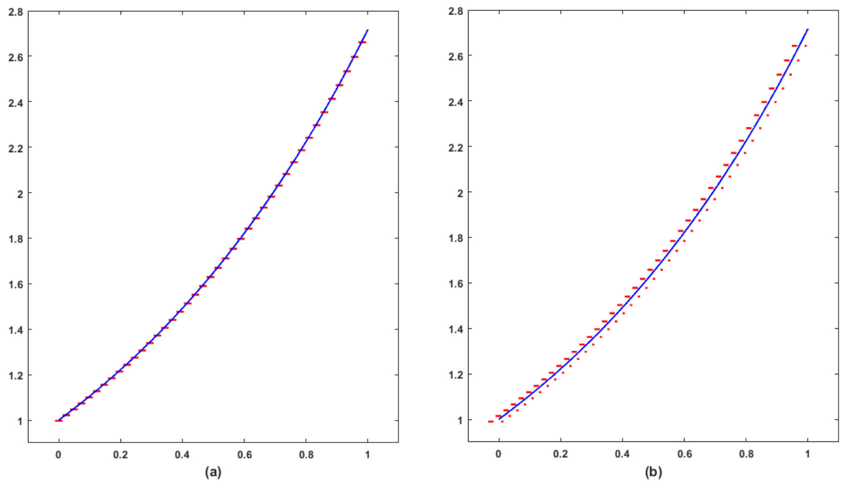

FIGURE 3. Comparison of the approximated solution (dashed red line) using ${}_{(0.3)}\hat{\Phi}_{m,8}$ and ${}_{(0.3)}\hat{\Psi}_{m,8}$ with the exact solution (blue line) (Example: 5.2).

5.2. Numerical solution for nonlinear Volterra integral equations. Consider the following nonlinear Volterra integral equation of the second kind,

$$u(t) = f(t) + \int_0^t K(t,s) \sum_{l=0}^{N} f_l(s) u^l(s) ds, \ N > 1, \tag{5.6}$$

where the functions $f, f_l \in L^2[0,1]$ and $K(t,s) \in L^2([0,1]\times[0,1])$ are given functions, $u(t)$ is unknown function and N is a positive integer. Here, we suppose that $K(t,s) = k_1(t)k_2(s)$. The proof is the same as the proof before Example 5.1, except that in the

Table 4: Rate of convergence for (Example: 5.2).

x	$\mathrm{R}_8(x)$	$\mathrm{R}_{10}(x)$	$\mathrm{R}_{12}(x)$	$\mathrm{R}_{14}(x)$	$\mathrm{R}_{16}(x)$
0.1	1.0804	1.0191	1.0148	1	1
0.2	1.0388	1.0073	0.9989	1	1
0.3	1.0256	1.0173	1.0007	1	1
0.4	1.0191	1.0089	1.0007	1	1
0.5	1.0152	0.9997	1.0004	1	1
0.6	1.0135	0.9969	1.0027	1	1
0.7	1.0102	1.0018	0.9996	1	1
0.8	1.0137	1.0023	1.0003	1	1
0.9	1.0163	1.0027	1.0002	1	1

last equations according to the relation (3.3) we have,

$$X^T{}_{(c)}\hat{\Psi}_{mk}(t) = F^T{}_{(c)}\hat{\Psi}_{mk}(t)+$$

$$\int_0^t K_1^T{}_{(c)}\hat{\Psi}_{mk}(t)\sum_{l=0}^{N}{}_{(c)}\hat{\Psi}^T_{mk}(s)\ diag\,(\omega K_2)\ \ diag\,(\omega F_l)\ \ diag\left(\omega^{l-1}\ X^{l-1}\right)Xds$$

$$= F^T{}_{(c)}\hat{\Psi}_{mk}(t) + \left(\int_0^t K_1^T{}_{(c)}\hat{\Psi}_{mk}(t)_{(c)}\hat{\Psi}^T_{mk}(s)ds\right)\times$$
$$\left(\sum_{l=0}^N diag\,(\omega K_2)\ \ diag\,(\omega F_l)\ \ diag\left(\omega^{l-1}\ X^{l-1}\right)X\right)$$

$$= F^T{}_{(c)}\hat{\Psi}_{mk}(t) + \left(K_1^T{}_{(c)}\hat{\Psi}_{mk}(t)_{(c)}\hat{\Psi}^T_{mk}(t)_{(c)}\hat{P}^T_{(m+1)}\right)\times$$

$$\left(\sum_{l=0}^N diag\,(\omega K_2)\ \ diag\,(\omega F_l)\ \ diag\left(\omega^{l-1}\ X^{l-1}\right)X\right)$$

$${}_{(c)}\hat{\Psi}^T_{mk}(t)X = {}_{(c)}\hat{\Psi}^T_{mk}(t)F + \left({}_{(c)}\hat{\Psi}^T_{mk}(t)\ diag\,(\omega K_1)\,{}_{(c)}\hat{P}^T_{(m+1)}\right)\times$$
$$\left(\sum_{l=0}^N diag\,(\omega K_2)\ \ diag\,(\omega F_l)\ \ diag\left(\omega^{l-1}\ X^{l-1}\right)X\right)$$

$$X = F + \left(diag\,(\omega K_2)\,{}_{(c)}\hat{P}^T_{(m+1)}\right)\times$$

$$\left(\sum_{l=0}^N diag\,(\omega K_2)\ \ diag\,(\omega F_l)\ \ diag\left(\omega^{l-1}\ X^{l-1}\right)X\right), \tag{5.7}$$

Eq. (5.7) is a system of nonlinear algebraic equations, with unknown vector X. We solve this nonlinear system by the Newton method and obtain u as $u \simeq X^T{}_{(c)}\hat{\Psi}_{mk}$. Note that the above method can be stated by basis vector (3.4).

Example 5.3. Consider the following nonlinear Volterra equation [24, 25],

$$u(t) - \int_0^t u^2(s)ds = sin(t) - \frac{t}{2} + \frac{1}{4}sin(2t), \tag{5.8}$$

the exact solution of this equation is $u(t) = sin(t)$. In Table 5, we compare our error approximations with the methods in [24, 25]. Fig. 4, (a) and (b) show the comparisons between the approximate solutions and exact solutions, when we used ${}_{(c)}\hat{\Phi}_{mk}$ and ${}_{(c)}\hat{\Psi}_{mk}$

in our method, respectively.

Table 5; Absolute error comparison of the present method with the methods in [24, 25] (Example: 5.3).

x	[24]	[25] $N=16$	New method by ${}_{(0.7)}\hat{\Psi}_{m,13}(x)$	New method by ${}_{(0.7)}\hat{\Phi}_{m,13}(x)$
0.1	3.33×10^{-4}	4.40×10^{-4}	4.73×10^{-4}	2.89×10^{-4}
0.2	1.54×10^{-3}	2.79×10^{-6}	5.70×10^{-4}	1.80×10^{-4}
0.3	6.65×10^{-3}	4.69×10^{-4}	6.30×10^{-4}	1.01×10^{-4}
0.4	1.39×10^{-2}	7.69×10^{-4}	3.66×10^{-4}	3.39×10^{-4}
0.5	0.00×10^{-2}	7.31×10^{-4}	6.04×10^{-4}	6.82×10^{-5}
0.6	4.70×10^{-2}	7.68×10^{-5}	4.56×10^{-4}	1.76×10^{-4}
0.7	6.90×10^{-2}	1.84×10^{-4}	3.86×10^{-4}	2.00×10^{-4}
0.8	9.59×10^{-2}	6.48×10^{-4}	5.13×10^{-4}	2.06×10^{-5}
0.9	1.43×10^{-1}	6.68×10^{-4}	2.75×10^{-4}	2.01×10^{-4}

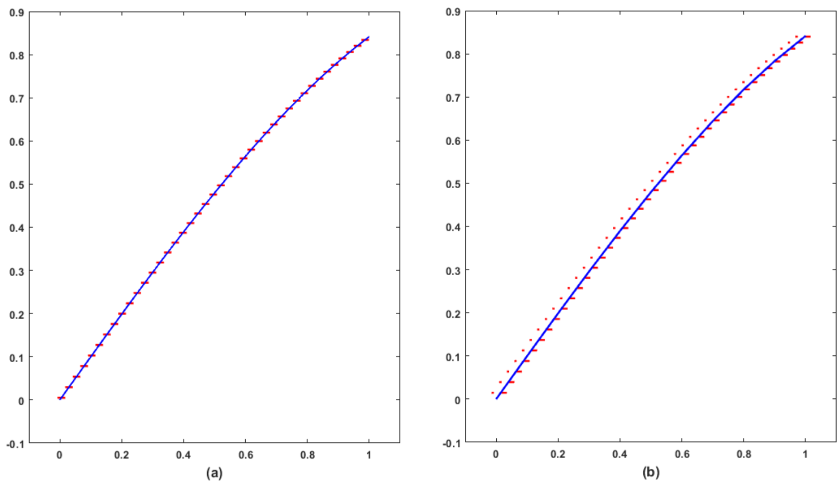

FIGURE 4. Comparison of the approximated solution (dashed red line) using ${}_{(0.7)}\hat{\Phi}_{m,8}$ and ${}_{(0.7)}\hat{\Psi}_{m,8}$ with the exact solution (blue line) (Example: 5.3).

Example 5.4. Consider the following nonlinear Volterra equation [25, 26],

$$u(t)+\int_0^t \big(u^2(s)+u(s)\big)\,ds=\frac{3}{2}-\frac{1}{2}e^{-2t}, \tag{5.9}$$

the exact solution of this equation is $u(t)=e^{-t}$. In Table 6, we compare our error approximations with the methods in [25, 26] and in Table 7, we compute the rate of convergence for some k. Fig. 5, (a) and (b) show the comparisons between the approximate solutions and exact solutions, when we used ${}_{(c)}\hat{\Phi}_{mk}$ and ${}_{(c)}\hat{\Psi}_{mk}$ in our method, respectively.

Table 6: Absolute error comparison of the present method with the methods in [25, 26] (Example: 5.4).

x	[26]	[25] $N = 16$	New method by ${}_{(0.5)}\hat{\Psi}_{m,16}(x)$	New method by ${}_{(0.5)}\hat{\Phi}_{m,16}(x)$
0.1	8.33×10^{-4}	2.33×10^{-4}	1.55×10^{-4}	6.84×10^{-5}
0.2	3.75×10^{-4}	1.28×10^{-5}	1.27×10^{-4}	4.86×10^{-5}
0.3	1.11×10^{-3}	4.25×10^{-4}	1.05×10^{-4}	3.42×10^{-5}
0.4	3.51×10^{-4}	3.64×10^{-7}	8.87×10^{-5}	2.35×10^{-5}
0.5	5.80×10^{-4}	1.19×10^{-4}	7.36×10^{-5}	1.54×10^{-5}
0.6	1.32×10^{-4}	7.97×10^{-6}	6.20×10^{-5}	9.40×10^{-6}
0.7	4.95×10^{-4}	2.41×10^{-4}	5.24×10^{-5}	4.79×10^{-6}
0.8	1.73×10^{-4}	2.74×10^{-5}	4.44×10^{-5}	1.28×10^{-6}
0.9	3.68×10^{-4}	2.56×10^{-4}	3.76×10^{-5}	1.41×10^{-6}

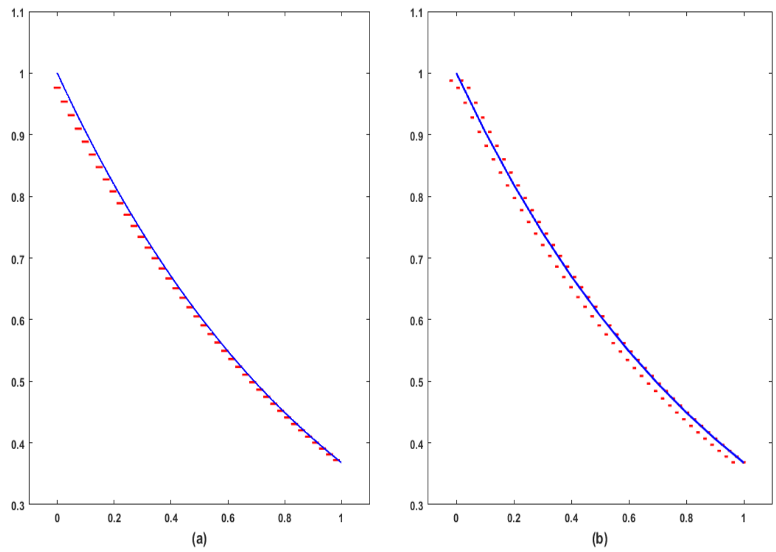

FIGURE 5. Comparison of the approximated solution (dashed red line) using ${}_{(0.5)}\hat{\Phi}_{m,8}$ and ${}_{(0.5)}\hat{\Psi}_{m,8}$ with the exact solution (blue line) (Example: 5.4).

Table 7; Rate of convergence for (Example: 5.4).

x	$\mathrm{R}_8(x)$	$\mathrm{R}_{10}(x)$	$\mathrm{R}_{12}(x)$	$\mathrm{R}_{14}(x)$	$\mathrm{R}_{16}(x)$
0.1	0.9418	0.9537	0.9731	1	1
0.2	0.8778	1.0091	0.9947	1	1
0.3	0.9570	1.0083	0.9969	1	1
0.4	0.9710	0.9775	1.0018	1	1
0.5	0.9791	0.9833	0.9986	1	1
0.6	0.9877	0.9959	0.9964	1	1
0.7	1.0224	0.9968	0.9993	1	1
0.8	1.0206	0.9982	0.9937	1	1
0.9	1.0153	1.0038	1.0008	1	1

References

[1] E. Babolian and A. Shahsavaran, Numerical solution of nonnliniear Fredholm integral equations of the second kind using Haar Wavelets, J. Comput. Appl. Math., 225 (2009), no. 1, 87–95.

[2] J. J. Benedetto and S. Sumetkijakan, *A fractal set constructed from class of wavelet sets*, Inverse Problems, Image Analysis, and Medical Imaging (New Orleans, LA, 2001), 19–35. Contemp. Math., 313, American Mathematical Society, Providence, RI, 2002.

[3] G. Capobianco, D. Conte and I. Del Prete, High performance parallel numerical methods for Volterra equations with weakly singular kernels, J. Comput. Appl. Math., 228 (2009), no. 2, 571–579.

[4] C. F. Chen and C. H. Hsiao, Haar wavelet method for solving umped and distributed-parameter system, IEEE Proc. Control Theory Appl., 144 (1997), 87–94.

[5] C. K. Chui, *An introduction to wavelets*, Academic Press, Boston, MA, 1992.

[6] X. Dai and D. R. Larson, Wandering vectors for unitary systems and orthogonal wavelets, Mem. Amer. Math. Soc., 134 (1998), no. 640, viii+68 pp.

[7] X. Dai, D. R. Larson, and D. M. Speegle, *Wavelet sets in* $\mathbb{R}^n$ *II*, Wavelets, multiwavelets, and their applications (San Diego, CA, 1997), 15–40, Contemp. Math., 216, American Mathematical Society, Providence, RI, 1998.

[8] X. Dai, and S. Lu, Wavelets in subspaces, Michigan Math. J., 43 (1996), 81–98.

[9] I. Daubechies, *Ten Lectures on Wavelets*, CBMS-NSF Regional Conf. Ser. in Appl. Math., 61, Society for Industrial and Applied Mathematics (SIAM), Philadelphia, PA, 1992.

[10] X. Fang and X. Wang, Construction of minimally supported frequency wavelets, J. Fourier Anal. Appl., 2 (1996), no. 4, 315–327.

[11] J. P. Gabardo and X. Yu, Construction of wavelet sets with certain self-similarity properties, J. Geom. Anal., 14 (2004), no. 4, 629–651.

[12] A. Golbabai and B. Keramati, Solution of non-linear Fredholm integral equations of the first kind using modified homotopy perturbation method, Chaos Solitons Fractals, 39 (2009), no. 5, 2316–2321.

[13] E. Hernández, X. Wang and G. Weiss, Smoothing minimally supported frequency wavelets: Part I, J. Fourier Anal. Appl., 2 (1996), no. 4, 329–340.

[14] E. Hernández and G. Weiss, *A first course on wavelets*, CRC Press, Boca Raton, FL, 1996.

[15] Siraj-ul-Islam, I. Aziz and A. S. Al-Fhaid, An improved method based on Haar wavelets for numerical solution of nonlinear integral and integro-differential equations of first and higher orders, J. Comput. Appl. Math., 260 (2014), 449–469.

[16] M. J. Kheirdeh, A. Askari Hemmat and H. saeedi, An application of s-elementary wavelets in solving differential and fractional integral equations numerically, J. Mahani Math. Res. Cent., 11 (2022), no. 3, 15–31.

[17] Ü. Lepik, Haar wavelet method for nonlinear integro-differential equations, Appl. Math. Comput., 176 (2006), no. 1, 324–333.

[18] Ü. Lepik, Application of the Haar wavelet transform to solving integral and differential equations, Proc. Estonian Acad. Sci. Phys. Math., 56 (2007), no. 1, 28–46.

[19] Ü. Lepik and H. Hein, *Haar wavelets: with applications*, Springer, Cham, 2014.

[20] J. Majak, M. Pohlak, K. Karjust, M. Eerme, J. Kurnitski, and B. S. Shvartsman, New higher order Haar wavelet method: application to FGM structures, Compos. Struct., 201 (2018), 72–78.

[21] J. Majak, B. Shvartsman, M. Ratas, D. Bassir, M. Pohlak, K. Karjust, and M. Eerme, Higher-order Haar wavelet method for vibration analysis of nanobeams, J. Mater. Today Commun., 25 (2020), Art. ID 101290, 6 pp.

[22] Y. Meyer, *Wavelets and Operators*, Cambridge Stud. Adv. Math., 37, Cambridge University Press, Cambridge, 1992.

[23] M. Ratas, A. Salupere and J. Majak, Solving nonlinear PDEs using the higher order Haar wavelet method on nonuniform and adaptive grids, Math. Model. Anal., 26 (2021), no. 1, 147–169.

[24] J. Saberi-Nadjafi and M. Heidari, Solving nonlinear integral equations in the Urysohn form by Newton-Kantorovich-quadrature method, Comput. Appl. Math. 60 (2010), no. 7, 2058–2065.

[25] M. H. A. Sathar, A. F. N. Rasedee, A. A. Ahmedov, and N. Bachok, Numerical solution of nonlinear Fredholm and Volterra integrals by Newton-Kantorovich and Haar wavelets methods, Symm., 12 (2020), no. 12, Paper No. 2034, 13 pp.

[26] M. Sabzevari, A review on "Numerical solution of nonlinear Volterra-Fredholm integral equations using hybrid of . . . " [Alexandria Eng. J. 52 (2013) 551–555], Alexandria Eng. J. 58 (2019), no. 3, 1099–1102.

[27] H. Saeedi, G. N. Chuev, Triangular functions for operational matrix of nonlinear fractional Volterra integral equations, J. Appl. Math. Comput., 49 (2015), no. 1-2, 213–232.

[28] F. Salehi, H. Saeedi and M. Mohseni Moghadam, A Hahn computational operational method for variable order fractional mobile–immobile advection-dispersion equation, Math. Sci. (Springer), 12 (2018), no. 2, 91–101.

[29] H. Saeedi, F. Samimi, He's homotopy perturbation method for nonlinear Fredholm integro-differential equations of fractional order], Int. J. Eng. Res. Appl., 2 (2012), no. 5, 52–56.

[30] M. Sorrenti, M. Di. Sciuva, J. Majak, and F. Auriemma, Static response and buckling loads of multilayered composite beams using the refined zigzag theory and higher-order Haar wavelet method, Mech. Compos. Mater., 57 (2021), no. 1, 18 pp.

[31] S. A. Yousefi and M. Razzaghi, Legendre wavelets method for the nonlinear Volterra-Fredholm integral equations, Math. Comput. Simulation, 70 (2005), no. 1, 1–8.

Appendix

Finally, two examples for the case of n=2 are presented for Theorem 9.2.

Examlpe A_1 :

For a fixed $g \in \mathbb{R}^+$, let $A^T = B = \begin{bmatrix} -g^{\frac{1}{2}} & 0 \\ 0 & g^{\frac{1}{2}} \end{bmatrix}$, and let

$$Q_1 = (\cup_0^\infty Y_i) \cup \left(\cup_0^\infty (Y_i^{'})\right),$$

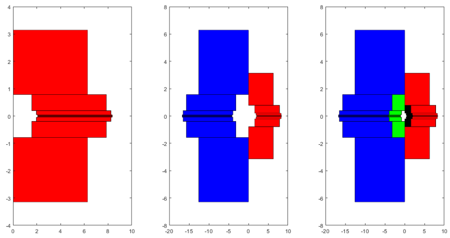

FIGURE 6. Q1 and its Dilations .

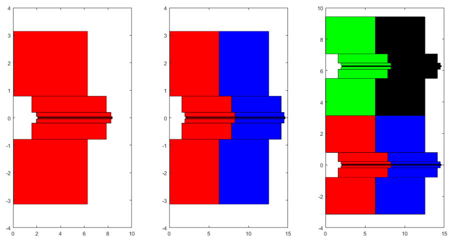

FIGURE 7. Q1 and its Translations.

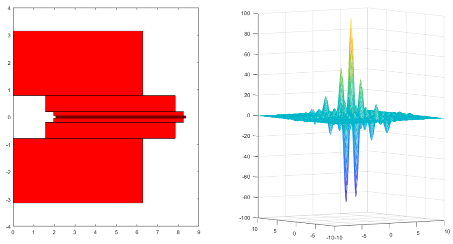

FIGURE 8. Q1 and its associated wavelet .

where

$$Y_0 = \operatorname{conv}\left\{(0,\pi),(0,\frac{\pi}{g}),(2\pi,\frac{\pi}{g}),(2\pi,\pi)\right\},$$

and$Y_i^{'}$ and Y_i are symmetric with respect $X-$axis and for for $i \geq 1$,

$$Y_i = \operatorname{conv}\{(\sum_{j=1}^{i}\frac{2\pi}{g^j},\frac{\pi}{g^i}),(\sum_{j=1}^{i}\frac{2\pi}{g^j},\frac{\pi}{g^{i+1}}),(2\pi+\sum_{j=1}^{i}\frac{2\pi}{g^j},\frac{\pi}{g^{i+1}}),(2\pi+\sum_{j=1}^{i}\frac{2\pi}{g^j},\frac{\pi}{g^i})\}.$$

Q_1 is a wavelet set. In particular,for $g=4$, see Figure 6, Figures 7 and Figure 8.

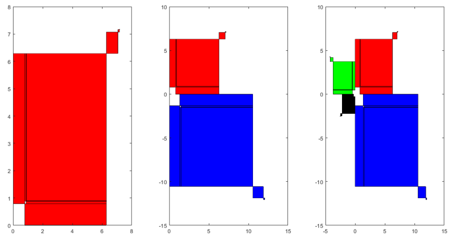

FIGURE 9. Q2 and its Dilations .

Examlpe A_2 :

For a fixed $g \in \mathbb{R}^+$, let $A^T = B = \begin{pmatrix} 0 & g^{\frac{1}{4}} \\ -g^{\frac{1}{4}} & 0 \end{pmatrix}$, where $g \in \mathcal{N}$ is fixed and let

$$Q_2 = (\bigcup_0^\infty Y_i) \bigcup (\bigcup_0^\infty Y_i^{'}) \bigcup Y \bigcup (\bigcup_0^\infty W_i),$$

where

$$Y = conv\{(\frac{2\pi}{g-1}, \frac{2\pi}{g-1}), (2\pi, \frac{2\pi}{g-1}), (2\pi, 2\pi), (\frac{2\pi}{g-1}, 2\pi)\},$$

$$Y_0 = conv\{(\frac{2\pi}{g}, 0), (2\pi, 0), (2\pi, \frac{2\pi}{g}), (\frac{2\pi}{g}, \frac{2\pi}{g})\},$$

$$w_0 = conv\{(2\pi + \frac{2\pi}{g}, (2\pi + \frac{2\pi}{g}), ((2\pi + \frac{2\pi}{g}, 2\pi), (2\pi, 2\pi + \frac{2\pi}{g}), (2\pi, 2\pi)\},$$

and for $i \geq 1$

$$Y_i = conv\{(\sum_{j=1}^{i+1} \frac{2\pi}{g^j}, \sum_{j=1}^{i} \frac{2\pi}{g^j}), (2\pi, \sum_{j=1}^{i} \frac{2\pi}{g^j}), (2\pi, \sum_{j=1}^{i+1} \frac{2\pi}{g^j}), (\sum_{j=1}^{i+1} \frac{2\pi}{g^j}, \sum_{j=1}^{i+1} \frac{2\pi}{g^j})\},$$

$$W_i = conv\{(2\pi + \sum_{j=1}^{i} \frac{2\pi}{g^j}, 2\pi + \sum_{j=1}^{i} \frac{2\pi}{g^j}), (2\pi + \sum_{j=1}^{i} \frac{2\pi}{g^j}, 2\pi + \sum_{j=1}^{i+1} \frac{2\pi}{g^j}),$$

$$(2\pi + \sum_{j=1}^{i+1} \frac{2\pi}{g^j}, 2\pi + \sum_{j=1}^{i+1} \frac{2\pi}{g^j}), (2\pi + \sum_{j=1}^{i+1} \frac{2\pi}{g^j}, 2\pi + \sum_{j=1}^{i} \frac{2\pi}{g^j})\}$$

and $Y_i^{'} = \{(x, y) : (y, x) \in Y_i\}$ for $i \geq 0$.

Q_2 is a wavelet set. In particular,for $g = 4$, see Figure 9, Figure 10 and Figure 11.

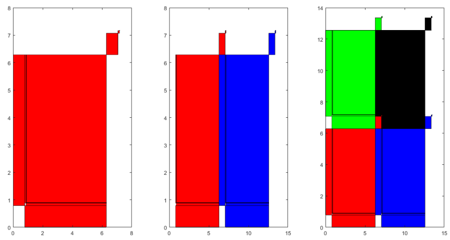

FIGURE 10. Q2 and its Translations.

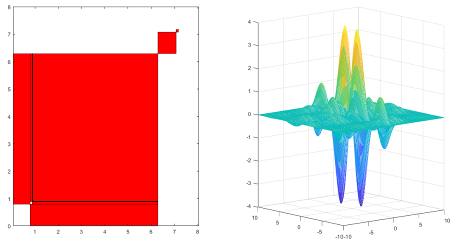

FIGURE 11. Q2 and its associated wavelet .

(M. J. Kheirdeh) DEPARTMENT OF MATHEMATICS, PAYAME NOOR UNIVERSITY (PNU), P.O.BOX 19395-4697, TEHRAN, IRAN.
E-mail address: `kheirdeh2@gmail.com`

(A. Askari Hemmat) DEPARTMENT OF APPLIED MATHEMATICS, FACULTY OF MATHEMATICS AND COMPUTER, SHAHID BAHONAR UNIVERSITY OF KERMAN, KERMAN, IRAN. TEMPRORY ADDRESS: DEPARTMENT OF MATHEMATICS AND STATISTICS, CONCORDIA UNIVERSITY, MONTREAL, CANADA
E-mail address: `askari@uk.ac.ir`

(H. Saeedi) DEPARTMENT OF APPLIED MATHEMATICS, FACULTY OF MATHEMATICS AND COMPUTER, SHAHID BAHONAR UNIVERSITY OF KERMAN, KERMAN, IRAN.
E-mail address: `saeedi@uk.ac.ir`